Characterization of 60GHz Millimeter-Wave Focusing Beam for Living-Body Exposure Experiments

Masaki KOUZAI[#1], Atsuhiro NISHIKATA[#*2], Taiji SAKAI[*3] and Soichi WATANABE[*4]
[#] *CRADLE, Tokyo Institute of Technology*
2-12-1-W9-109, Ookayama, Meguro-ku, Tokyo, 152-8552, Japan
[*] *National Institute of Information and Communications Technology*
4-2-1 Nukui-Kitamachi, Koganei-shi, Tokyo, 184-8795, Japan

***Abstract*— In this paper, a precise characterization of focusing beam is performed based on the field distribution measurement and beam reconstruction analysis, in order to enable detailed calculation of focusing beam exposure on the surface of human's skin. To estimate the influence of the experimental condition, we calculated electromagnetic field with varying parameters such as the distance, incident angle. The result suggests that the influence of positioning error is relatively small.**
Key words: millimeter wave, lens antenna, electromagnetic field, exposure calculation

I. Introduction

Recently, as the increasing use of millimeter-waves is expected, the anxiety is pronounced about increasing chance for general public to be exposed to millimeter-waves. It is necessary to prevent the adverse effect of millimeter-waves on the living body. The safety guidelines for millimeter-wave are provided [1], [2], [3]. The established mechanism by which the millimeter-waves have influence on living bodies is the thermal effect. Though there have been some investigations for thermal effect of millimeter-wave exposure[4], [5], [6], the experimental knowledge about the thermal sensation phenomena is still insufficient.

II. Analysis of Focusing Beam

A. Electromagnetic field in the free space

Electromagnetic field radiated from a lens antenna focuses with propagation, and mostly concentrates on the beam waist. Therefore, if the field distribution on the plane perpendicular to propagation direction is measured, the majority of power can be covered. We will estimate a beam profile from this field distribution. For convinience' sake, we assume that the measured plane is at $z = 0$, the source (lens antenna) is located on $z < 0$, and beam is of single frequency.

Assume that the electromagnetic field radiated by the source on $z < 0$ is measured on xy-plane, and x- and y-component of elctric field is obtained. We define $\tilde{E_x}(k_x, k_y)$ as a 2-dimentional Fourier-transform of $E_x(x, y, 0)$, Fourier-transform and inverse Fourier-transform is represented as

$$\tilde{E_x}(k_x, k_y) = \iint E_x(x, y, 0) e^{j(k_x x + k_y y)} dx dy, \quad (1)$$

$$E_x(x, y, 0) = \frac{1}{(2\pi)^2} \iint \tilde{E_x}(k_x, k_y) e^{-j(k_x x + k_y y)} dk_x dk_y. \quad (2)$$

The integration range is $(-\infty, \infty)$ for every variable and omitted in the expression. Here, the right hand of eq. (2) is considered as the value of plane-wave

$$\tilde{E_x}(k_x, k_y) e^{-j(k_x x + k_y y + k_{0z} z)} \quad (3)$$

$$k_{0z} = \sqrt{k_0^2 - k_x^2 - k_y^2} \quad (4)$$

on $z = 0$. The vector electric field with other component will be written as

$$\left(\hat{\boldsymbol{x}} - \frac{k_x}{k_{0z}} \hat{\boldsymbol{z}} \right) \tilde{E_x}(k_x, k_y) e^{-j(k_x x + k_y y + k_{0z} z)}. \quad (5)$$

Here, $\hat{\boldsymbol{x}}, \hat{\boldsymbol{y}}, \hat{\boldsymbol{z}}$ represent the fundamental vectors. Similarly, y-component can be calculated, and electric field is expressed as

$$\boldsymbol{E}(x, y, z) = \frac{1}{(2\pi)^2} \iint \left\{ \left(\hat{\boldsymbol{x}} - \frac{k_x}{k_{0z}} \hat{\boldsymbol{z}} \right) \tilde{E_x} + \left(\hat{\boldsymbol{y}} - \frac{k_y}{k_{0z}} \hat{\boldsymbol{z}} \right) \tilde{E_y} \right\} e^{-j(k_x x + k_y y + k_{0z} z)} dk_x dk_y. \quad (6)$$

Next, let us separate the electric field in TE(transverse electric)- and TM(transverse magnetic)-waves.

$$\boldsymbol{E} = \frac{1}{(2\pi)^2} \iint \left[\boldsymbol{p} f_{\mathrm{TE}} + \left(\boldsymbol{q} - \frac{k_t}{k_{0z}} \hat{\boldsymbol{z}} \right) f_{\mathrm{TM}} \right] e^{-j \boldsymbol{k}_0^+ \cdot \boldsymbol{r}} dk_x dk_y \quad (7)$$

The first term in the [ ] represents the TE-wave, and the second term represet the TM-wave. $\boldsymbol{p}$ and $\boldsymbol{q}$ are orthogonal unit vectors on xy-plane.

$$\boldsymbol{p} = \frac{k_y}{k_t} \hat{\boldsymbol{x}} - \frac{k_x}{k_t} \hat{\boldsymbol{y}} \quad (8)$$

$$\boldsymbol{q} = \frac{k_x}{k_t} \hat{\boldsymbol{x}} + \frac{k_y}{k_t} \hat{\boldsymbol{y}} \quad (9)$$

$$k_t = \sqrt{k_x^2 + k_y^2} \quad (10)$$

$\boldsymbol{r}$ is the position vector, $\boldsymbol{k}_0^+$ is the wave-number vector in the free space

$$\boldsymbol{k}_0^+ = k_x\hat{\boldsymbol{x}} + k_y\hat{\boldsymbol{y}} + k_{0z}\hat{\boldsymbol{z}} \quad (11)$$

$$k_{0z} = \sqrt{k_0^2 - k_t^2}. \quad (12)$$

$f_{\mathrm{TE}}, f_{\mathrm{TM}}$ are calculated from equations below.

$$f_{\mathrm{TE}} = \boldsymbol{p}\cdot\tilde{\boldsymbol{E}}_t = \frac{k_y}{k_t}\tilde{E}_x - \frac{k_x}{k_t}\tilde{E}_y \quad (13)$$

$$f_{\mathrm{TM}} = \boldsymbol{q}\cdot\tilde{\boldsymbol{E}}_t = \frac{k_x}{k_t}\tilde{E}_x + \frac{k_y}{k_t}\tilde{E}_y. \quad (14)$$

Next, for the analysis of the living body exposed to the millimeter-wave beam, we assume the multi-layered medium (N-layers) on $z \geq z_1$. For each $n = 1, \cdots, N$, the n-th layer has the complex relative permittivity ε_{rn}, and convers $z_n \leq z < z_{n+1}$. The N-th layer is semi-infinite ($z_{N+1} = \infty$), and every layer has relative permeability $\mu_r = 1$. Eq. (7) is expanded so that it includes backward wave, electromagnetic field in the n-th layer is calculated as

$$\begin{aligned}
\left\{ \begin{array}{c} \boldsymbol{E} \\ \boldsymbol{H} \end{array} \right\} = & \\
& \frac{1}{(2\pi)^2}\iint \left[a_{n\mathrm{TE}} \left\{ \begin{array}{c} \boldsymbol{p} \\ Z_{n\mathrm{TE}}^{-1}\left(\boldsymbol{q} - \frac{k_t}{k_{nz}}\hat{\boldsymbol{z}}\right) \end{array} \right\} f_{\mathrm{TE}} \right. \\
& \left. + a_{n\mathrm{TM}} \left\{ \begin{array}{c} \boldsymbol{q} - \frac{k_t}{k_{nz}}\hat{\boldsymbol{z}} \\ Z_{n\mathrm{TM}}^{-1}(-\boldsymbol{p}) \end{array} \right\} f_{\mathrm{TM}} \right] \cdot \\
& e^{-j\boldsymbol{k}_n^+\cdot(\boldsymbol{r} - z_n\hat{\boldsymbol{z}})} dk_x dk_y + \\
& \frac{1}{(2\pi)^2}\iint \left[b_{n\mathrm{TE}} \left\{ \begin{array}{c} \boldsymbol{p} \\ Z_{n\mathrm{TE}}^{-1}\left(-\boldsymbol{q} - \frac{k_t}{k_{nz}}\hat{\boldsymbol{z}}\right) \end{array} \right\} f_{\mathrm{TE}} \right. \\
& \left. + b_{n\mathrm{TM}} \left\{ \begin{array}{c} \boldsymbol{q} + \frac{k_t}{k_{nz}}\hat{\boldsymbol{z}} \\ Z_{n\mathrm{TM}}^{-1}\boldsymbol{p} \end{array} \right\} f_{\mathrm{TM}} \right] \cdot \\
& e^{-j\boldsymbol{k}_n^-\cdot(\boldsymbol{r} - z_{n+1}\hat{\boldsymbol{z}})} dk_x dk_y, \\
& z_n < z < z_{n+1}, \quad n = 1, \cdots, N, \quad (15)
\end{aligned}$$

$$k_{nz} = \sqrt{k_0^2\varepsilon_{rn} - k_t^2} \quad (16)$$

$$\boldsymbol{k}_n^{\pm} = k_x\hat{\boldsymbol{x}} + k_y\hat{\boldsymbol{y}} \pm k_{nz}\hat{\boldsymbol{z}} \quad (17)$$

$$Z_{n\mathrm{TE}} = \eta_0\frac{k_0}{k_{nz}} \quad (18)$$

$$Z_{n\mathrm{TM}} = \eta_0\frac{k_{nz}}{k_0\varepsilon_{rn}} \quad (19)$$

$$\eta_0 = \sqrt{\frac{\mu_0}{\varepsilon_0}} \quad (20)$$

III. Field Measurement

We measured the amplitude and phase of electric field radiated from millimeter-wave lens antenna by using Near-field measurement system. Figure 1 shows two kinds of lens antennas under test, and its frequency is 60GHz.

As shown in Figure 2, the open-ended waveguide probe is located in front of lens antenna under test. We defined the coordinate axes, such that z-axis is beam propagation direction, x-axis is horizontal, and y-axis is vertical direction. Electromagnetic wave radiated from lens antenna is mainly horizontally-polarized wave.

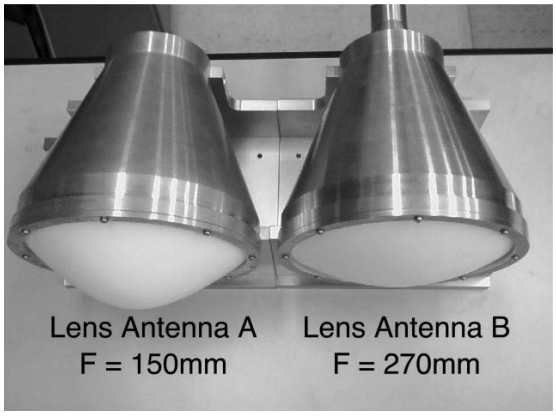

Fig. 1. Two kinds of lens antennas under test.

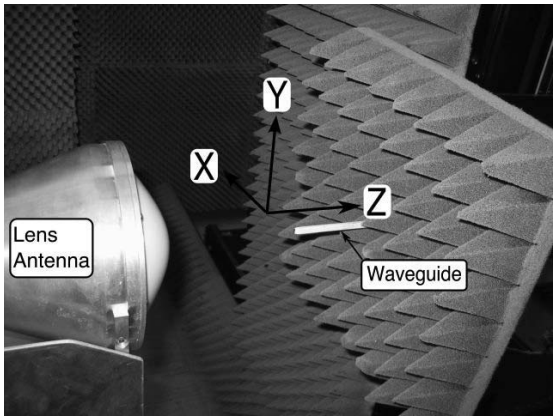

Fig. 2. Near-field measurement system.

Table I shows the measurement condition. Figure 3 shows the field intensity E_x and E_y measured on xy-plane. It can be seen that E_x focuses elliptically, and the maximum value of E_y is less than that of E_x by 20dB. Here we defined 0dB as the maximum value of $|E_x|$ on measured plane.

TABLE I
MEASUREMENT CONDITIONS OF TWO KINDS OF LENS ANTENNAS

Lens antenna	A	B
F	150mm	270mm
Measurement interval($\Delta x, \Delta y$)	1mm	2mm
Measurement area	100mm× 100mm	200mm× 200mm
Measurement plane (z)	0, ±10, ±50mm	0, ±10mm

IV. Calculation Results

A. Reconstruction in free space

The electric field distribution of millimeter-wave beam is reconstructed from measured E_t. Namely, $\boldsymbol{E}(x, y, z)$ on

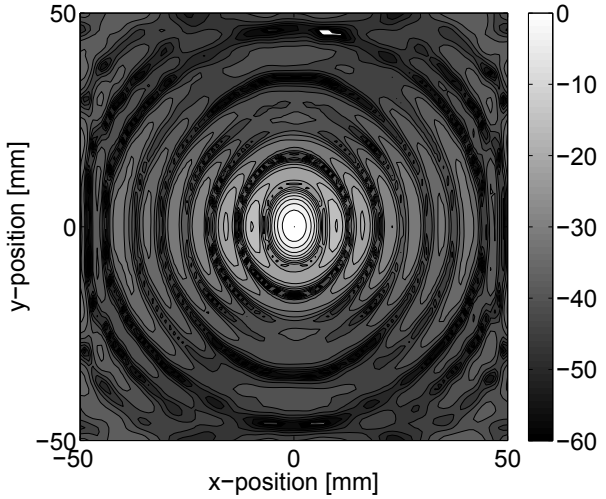

(a) E_x intensity in decibel

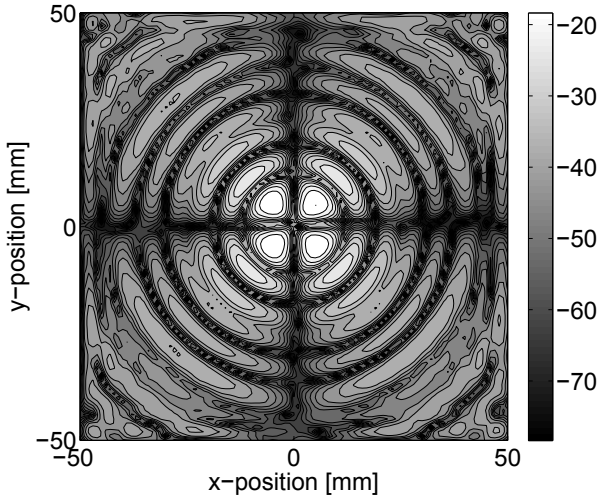

(b) E_y intensity in decibel

Fig. 3. Field E_x or E_y's intensity of lens antenna A measured on xy plane.

arbitrary z is calculated from $\boldsymbol{E}_t(x, y, 0)$. Figure 4 shows the beam profile of lens antennas. For each cross-section, the field intensity distribution is normalized with the maximum value. It can be seen that the lens antenna A has larger focusing angle and narrower beam waist than lens antenna B. Figure 5 shows the reconstructed field intensity distribution on xz-plane, especially around the focus. We defined $0\mathrm{dB}$ as the maximum value in the calculation area, and uses this definition in the following figures. It can be seen that the lens antenna A has less uniformity along z-axis. The half-width spheroidal area has different lengths for each directions. The half-width length for each axis is shown in Table II.

TABLE II

HALF-WIDTH OF ELECTRIC FIELD INTENSITY FOR EACH AXIS.

	$x[\mathrm{mm}]$	$y[\mathrm{mm}]$	$z[\mathrm{mm}]$
Antenna A	5.7	7.5	52.2
Antenna B	9.9	12.9	122.9

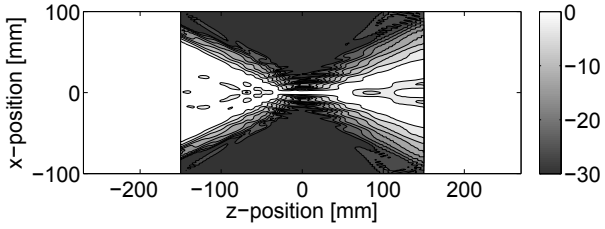

(a) Antenna A

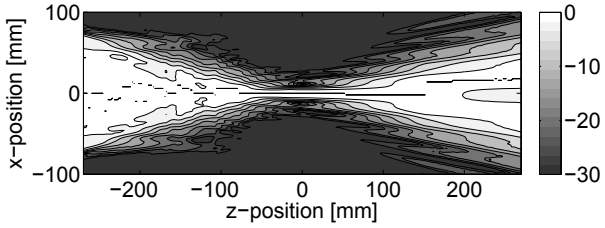

(b) Antenna B

Fig. 4. Reconstructed field intensity on xz-plane.

B. Incidence to living-body model

We modelled the living body as a two-layered object which has skin layer and fat layer, and calculated the electromagnetic field when exposed to millimeter-wave focusing beam. The skin layer has finite thickness, and the fat layer has semi-infinite thickness. In addition, we calculated on the three-layered model with muscle. Since there is little difference in the result, we adopt two-layered model. Table III shows relative permittivity and loss tangent of body tissues used in calculation. These parameters are obtained by estimation formula [7].

TABLE III

BODY TISSUES' PARAMETERS AT 60GHZ.

tissue	relative permittivity(ε_r)	loss tangent ($\tan\delta$)
Skin (dry)	7.98	1.37
Skin (wet)	10.2	1.16
Fat	3.13	0.27
Muscle	12.9	1.23

On millimeter-wave exposure experiment, it is difficult to keep exposing in an ideal condition. Therefore, to estimate the influence of the difference of the experimental condition, we calculated electromagnetic field with varying the skin surface position, incidence angle, skin moisture and thickness of skin.

1) skin surface position: Figure 6 shows peak field intensity in the skin when the skin surface position varies in z-direction. Lens-antenna A's variation is strongly asymmetric with respect to $z = 0$, and rapidly declines when skin surface moves away from the focus. On the other hand, lens antenna B having longer focal length has gradual charasteristics. For example, the positioning error of $\pm 5\mathrm{mm}$ shall result in 0.8dB deviation for lens antenna A and 0.1dB for lens antenna B. Table IV shows the maximum value of field intensity and powerdensity in freespace, and SAR in the skin when incident power is normalized to 1W for each lens antenna. Here, the value of

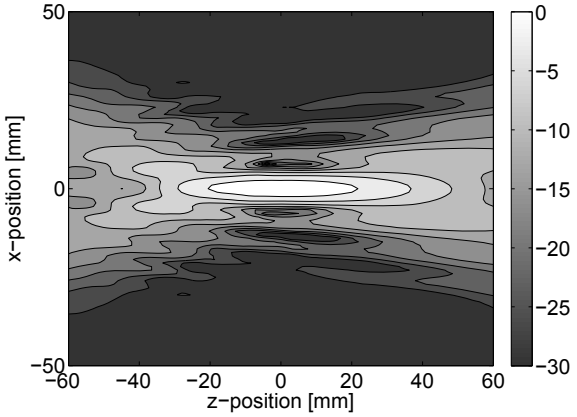

(a) Antenna A

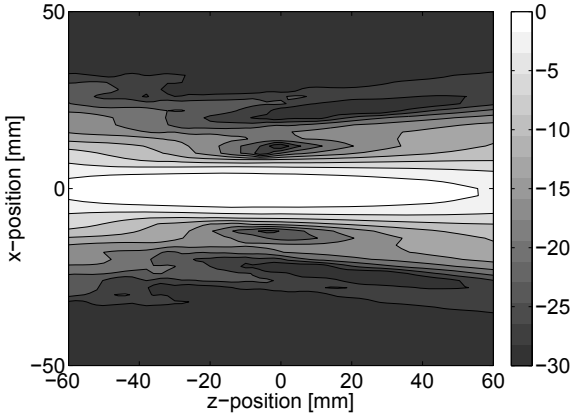

(b) Antenna B

Fig. 5. Reconstructed field intensity on xz-plane around focus.

TABLE IV

MAXIMUM VALUES OF FIELD INTENSITY, POWER DENSITY AND SAR AT FOCUS, WHEN INCIDENT POWER IS NORMALIZED TO 1W.

Lens antenna	A	B
Maximum field intensity $E\max[\mathrm{V/m}]$	2.65×10^3	1.62×10^3
Maximum power density $P\max[\mathrm{mW/cm^2}]$	1.86×10^3	6.98×10^2
Maximum SAR[W/kg]	4.74×10^4	1.78×10^4

SAR includes no spatial averaging.

2) oblique incidence: Figure 7 shows peak field intensity at the skin surface when the incident angle increases. There is a significant difference between two rotation axis. When rotating around y-axis, the electromagnetic wave is considerd as quasi-TM incidence, and around x-axis as quasi-TE incidence. Variation is higher for quasi-TE-incidence case. It can be seen that the peak $|E|$ declines only 0.2dB if the angle is controlled within ± 10 degrees.

V. CONCLUSION

The electromagnetic field analysis of the millimeter-wave focusing beam exposure experiment was performed. We can say that the positioning error and skin condition change shall result in the difference of $|E|$ less than 1dB. As a future work, we will perform the thermal sensation threshold experiment to clarify the thermal sensation dependency of duration, exposure area, and exposure position.

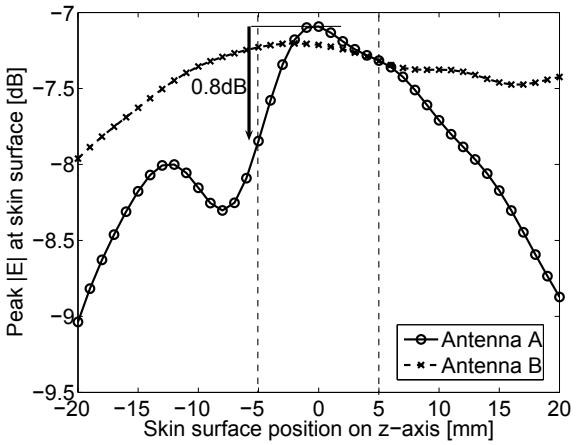

Fig. 6. Changes in Peak field intensity for skin surface position.

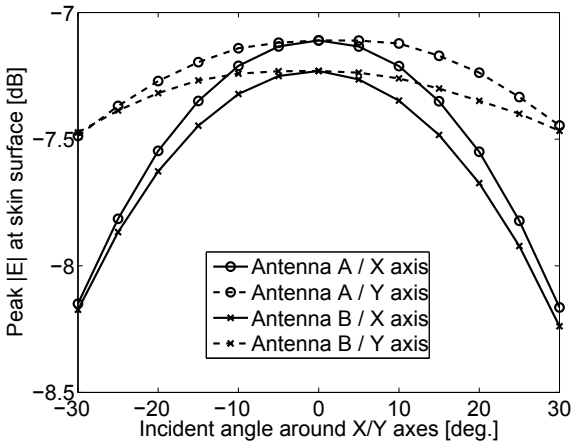

Fig. 7. Changes in Peak field intensity for oblique incidence.

REFERENCES

[1] International Commission on Non-Ionizing Radiation Protection, "Guidelines for limiting exposure to time-varying electric, magnetic, and electromagnetic fields (up to 300 GHz)," 1998.

[2] IEEE Std C95.1, "IEEE Standard for Safety Levels with Respect to Human Exposure to Radio Frequency Electromagnetic Fields, 3 kHz to 300 GHz."

[3] Telecommunication Technology Council, "Radio-Radiation Protection Guidelines for Human Exposure to Electromagnetic Fields", TTC Report No.38 (1990) (in Japanese).

[4] O. P. Gandhi and A. Riazi, Absorption of Millimeter Waves by Human Beings and its Biological Implications, *IEEE Trans. Microwave Theory Tech.*, vol.MTT-34, no.2, 1986, 228-235.

[5] F. Gustrau and A. Bahr, W-Band Investigation of Material Parameters, SAR Distribution, and Thermal Response in Human Tissue, *IEEE Trans. Microwave Theory Tech.*, vol.MTT-50, No.10, 2002, 2393-2400.

[6] T. Konno *et al.*, A Fundamental Study of Warmth Sensation Produced by Millimeter-Wave Exposure, *IEICE technical meeting of EMCJ*, vol.104, no.150, Hokkaido, Japan, 2004, 61-66.

[7] S.Gabriel, R.W.Lau and C.Gabriel: "The dielectric properties of biological tissues: III. Parametric models for the dielectric spectrum of tissues", Phys. Med. Biol. 41, pp.2271-2293 (1996).